HEFAT2014
10th International Conference on Heat Transfer, Fluid Mechanics and Thermodynamics
14 – 16 July 2014
Orlando, Florida

NUMERICAL ANALYSIS OF HEAT TRANSFER INCREASE IN A TUBE WITH ALTERNATE SUCCESSIVE GRADUAL WALL DEFORMATIONS

Zambaux J. A.[1,2,3]*, Russeil S.[1,2], Harion J. L.[1,2] and Bouvier P.[1,2,3]
*Author for correspondence
[1] EI, Mines Douai,
Douai, F-59500, France,
[2] Université Lille Nord de France,
Lille, F-59000, France,
[3] EEA Department, HEI,
Lille, F-59046, France,
E-mail: julie-anne.zambaux@mines-douai.fr

ABSTRACT

From previous studies, it is known that the use of wall deformations in alternate directions while keeping a quasi-constant cross-section is an efficient way to enhance the heat transfer in a laminar flow regime inside a tube. In the present study, the tube cross-section shape gradually changes along the tube length while keeping the same cross-sectional area to prevent flow separation areas thereby limiting pressure drops. These wall deformations create vortical macrostructures inside the flow that significantly modify the transfer properties. Two geometrical parameters characterize the tube wall shape: the radial deformation amplitude and its streamwise wavelength. Through a numerical study, the effects of the variation of these two parameters on the flow and on the heat transfer have been studied. An important finding is that the ratio between the wavelength and the amplitude has a significant impact on the observed results: both the friction and the heat transfer increases as this deformation ratio decreases. At the same time, a local analysis of the flow mechanisms has been performed to outline the modifications that occur in the flow pattern when the wall deformations are increased. Flow in the entrance region has also been specifically considered: it has been found that geometrical parameters do have an influence on the length needed for the flow to get fully hydrodynamically and thermally established. Finally a performance analysis has been conducted to assess, for a given performance criterion, the deformation parameters that give optimal results. Through this parametric study, for the given Reynolds and Prandtl numbers, an alternate wall deformed tube geometry that maximizes the heat transfer without significantly increasing the pressure drops can thus be defined.

NOMENCLATURE

A	[%]	Maximum radius increase of the tube	
R	[m]	Mean tube radius	
T	[K]	Fluid temperature	
X	[m]	Coordinate in the flow direction	
ΔP	[Pa]	Pressure drop	
L	[m]	Tube total length	
u_m	[m/s]	Mean velocity	
h	[W/m²K]	Convective heat transfer coefficient	
k	[W/mK]	Thermal conductivity	
Cp	[J/kgK]	Specific heat	
f	[-]	Friction coefficient	$f = \frac{2R\Delta P}{L\frac{1}{2}\rho u_m^2}$
Nu	[-]	Nusselt number	$Nu = \frac{2Rh}{k}$
Re	[-]	Reynolds number	$\mathrm{Re} = \frac{\rho 2Ru_m}{\mu}$
Pr	[-]	Prandtl number	$\mathrm{Pr} = \frac{\mu C_p}{k}$
Sc	[-]	Schmidt number	$Sc = \frac{\mu}{\rho \mathcal{D}}$

Special characters

η	[-]	Heat transfer efficiency
λ	[-]	Non dimensional deformation wavelength
τ	[s]	Mixing characteristic time
ρ	[kg/m³]	Density
μ	[kg/ms]	Dynamic viscosity
$\mathcal{D}$	[m²/s]	Molecular diffusion coefficient

Subscripts

0	Smooth reference tube
def	Deformed tube
W	Wall
th	Theoretical value

INTRODUCTION

More efficient use of energy has been a growing issue over the past years. In that framework, many developments to improve heat exchangers have been achieved. To enhance heat transfer efficiency is one of the major issues related to this topic. In order to improve the heat transfer, one solution consists of increasing the convection within the exchanger. Inner flows must be perturbed to modify the transfer behaviour. Enhancement techniques can be cast into two main categories: active solutions, which use an external source of energy to modify the flow characteristics and increase the convective heat transfer (see for example pulsatile flows [1] or the use of electrostatic fields [2]), and passive methods, which use the device geometry itself to modify the flow structure. This last kind of technique can be particularly useful since it can help increase the heat transfer with limited pumping power needed. Numerous passive methods can be used for low Reynolds numbers flows. To enhance the heat transfer of inner flows through passive ways, several tube geometric elements can be used such as bends [3, 4, 5] or inserts [2] like mixing tabs [6, 7] or twisted tape inserts [8]. Deforming the tube wall can also help improve the transfer properties of the flow. Corrugated tubes are already widely used in industry and have been the subject of many experimental and numerical studies reported in the literature. For a laminar regime, these tubes have been specifically studied by Rainieri et al. [9, 10, 11]. Even if heat transfer can be enhanced by corrugated tubes, significant penalties are induced. Pressure drops may indeed be large especially if a tubes cross-sectional area changes. A reduction of this area implies an augmentation of the flow velocity and thus of the pressure drops. The variations of the cross-sectional area may also induce recirculation zones inside the tube as it was shown by Mahmud et al. [12] for tubes with a sinusoidally deformed wall. Therefore some authors have tried to prevent the formation of reverse flow areas and to reduce the increase of pressure drop in tubes with varying cross-sections by attempting to keep their area constant or, at least, nearly constant. One can cite the helically twisted tube with an elliptic cross-section (Bishara et al. [13]) or the tube with alternate elliptic deformation of its cross-section presented by Meng et al. [14] and Chen et al. [15, 16, 17]. For low Reynolds numbers, this alternate elliptic tube improves the heat transfer significantly. The deformed tube presented by Harion et al. [18] is built while keeping the cross-sectional area nearly constant and by changing gradually and periodically its shape from elliptic to circular along the axial length. Comparatively with the above-mentioned tubes, the wall deformation is smoother. Better hydrodynamical properties can therefore be expected for this tube. The current paper studies the performance of this particular tube. Through numerical simulations, the best tube deformation parameters are studied. The performance criterion chosen to assess the device performance is the efficiency defined by the ratio between the Nusselt number and the friction coefficient for the deformed tube and a reference smooth tube (see equation (1)):

$$\eta = \frac{Nu / Nu_0}{f / f_0} \qquad (1)$$

One of the main aims of the current paper is to study the performance achieved by a deformed tube and its evolution when the deformation parameters vary. Firstly a study of the local flow pattern is provided to give a better understanding of the heat transfer mechanisms. The influence of the entrance length on the tube performance is also discussed.

TUBE CONFIGURATION

Tube Geometry

The tube geometry presented in this paper was proposed by Harion et al. [18]. In order to prevent recirculation zones from appearing in the flow, the tube cross-sectional area remains constant (or nearly constant). The heat transfer enhancement is achieved by deforming the tube wall to create stretching and compression phenomena in the radial direction of the flow. The wall deformation is applied to a smooth circular tube of radius R. Figure 1 gives the deformation principle. It is made of a periodical succession of deformed parts in the flow direction. For each part, the circular cross-section becomes elliptic before repeating its original shape. Two geometrical parameters can be defined to describe the wall deformation: the amplitude A and the wavelength parameter λ. As it is shown in Figure 1, AR represents the maximum elliptic length compared with the radius R of the smooth circular tube. The physical wavelength of the deformation is λR.

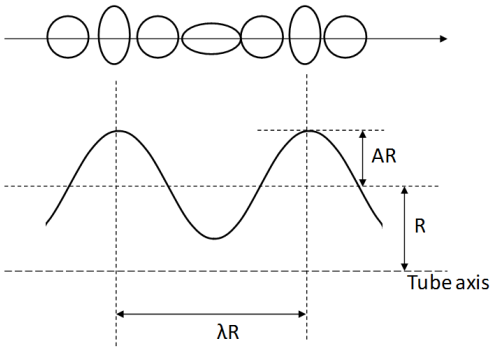

Figure 1 Deformed Tube geometry

Several experimental tests were already performed on the deformed tube [18]. Pressure drops were measured and heat transfer coefficients were calculated over a large range of Reynolds numbers. Through this experimental study, it was shown that the deformed tube enhances heat transfer in the laminar regime (below *Re=3000* with the experimental set-up described in [18]). The average efficiency η is found to be *1.2*. For higher Reynolds number flows, turbulence controls the heat transfer mechanisms. Therefore, the tube wall deformation only bears a small influence on the global results. In the following section, the deformed tube will hence be studied in the laminar regime where it can help increasing the heat transfer significantly.

Deformation Parameters and Mixing Time

The heat transfer and flow characteristics depend on the wall deformation applied to the tube. Parameters A and λ do

have a significant effect on the transfer phenomena within the tube. More precisely, Harion et al. [18] have shown that it is in fact the ratio λ/A that seems to control the tube performances. They compared the mixing characteristic time in the deformed tube τ_{def} (radial mixing) and in a smooth reference tube τ_0 (pure diffusive mixing). The relation given in equation (2) was proposed:

$$\frac{\tau_{def}}{\tau_0} \alpha \frac{\lambda}{A} \frac{1}{Sc\,\mathrm{Re}} \qquad (2)$$

The mixture characteristic time τ_{def} depends on the fluid and flow properties but also on the device geometric parameters A and λ. Therefore, according to equation (2), for a given fluid flow, the deformation ratio λ/A is the only parameter ruling the mixing of the flow and consequently the convective heat transfer in the tube. If λ/A is to increase, mixing time in the deformed tube also increases and thus, heat transfer decreases.

NUMERICAL SETTINGS

The simulations were performed using the CFD code ANSYS Fluent v12.0. The mass and momentum conservation equations were solved with the energy equation. The discretization schemes used were second order upwind for the energy and momentum, standard for the pressure. To solve the velocity and pressure coupling, the SIMPLEC algorithm was used. All the simulations were carried out for a steady incompressible flow in the laminar regime.

The fluid that flows inside the tube is a mixture of *30%* glycol and water. Since the maximum temperature range considered remains small, the fluid thermo-physical properties variation can be neglected. The Prandtl number of the fluid is $Pr=9.64$.

To ensure that the results were converged, residuals were closely monitored and the global heat transfer balance was verified. The pressure, velocity and temperature trends were also checked locally during the iteration process by monitoring their successive values at one given point, for each iteration. The monitored point was chosen near the end of the tube. At the end of the calculation, asymptotic behaviour was achieved for the observed quantities.

At the inlet of the tube, a fully developed velocity profile was applied. It was obtained from primary simulations of the inner flow in a smooth tube long enough to get an established flow regime. The Reynolds number calculated using the mean tube diameter ($2R$) and the mean velocity is $Re = 828$. The inlet temperature value was fixed at $321.3K$. At the outlet of the tube, the longitudinal gradient terms were set to zero. As for the boundary conditions applied to the wall, a no slip condition was imposed. Concerning the energy equation, a fixed temperature boundary condition $T_W=299K$ was set on the wall.

Mesh and Grid Sensitivity Study

The software GAMBIT was used to build the tube geometry and mesh. The entrance face was meshed and then extruded along the tube axial length. This method allowed getting a 3D hexahedral mesh with similar cell sizes and aspect ratios. Near the tube wall, the mesh density was refined to calculate the wall gradients accurately. Figure 2(a) shows the mesh generated for the entrance face. Figure 2(b) shows the mesh of an example of deformed tube, generated over one period. The quality of the generated mesh was closely verified for all the simulations: the cell skewness (which assesses how close to an ideal cell the studied cell is, see [19]), was determined. For all the meshes its maximum value (observed for the largest deformation amplitude case) remains lower than *0.7*, which corresponds to a mesh with a fair enough quality, while the mean skewness value is around *0.35* (meaning a good mesh quality). For more moderate deformation amplitude, the maximum skewness lowers to values below *0.5* and the mean skewness remains below *0.2*, thereby ensuring a quite good mesh quality for most of the cases.

Each tube has a mean radius $R=5mm$ and was studied over a global length $L=420mm$. Different deformation wavelengths and amplitudes were considered.

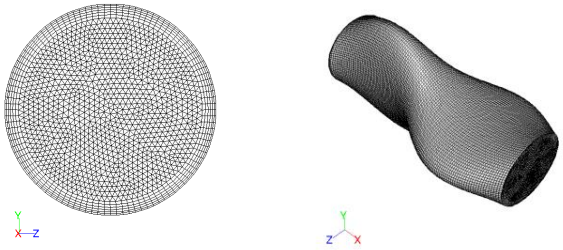

(a) Mesh of the entrance face (b) Three-dimensional grid for A=60% and λ=6 (one period)

Figure 2 Deformed Tube grid

A grid sensitivity study was performed to find the most appropriate mesh size that gives satisfactory results. The geometry configuration chosen to perform the analysis is the most severely deformed with an amplitude $A=60\%$ and a wavelength $\lambda=6$. The tube was studied over twelve periods. Table 1 sums up the characteristics of the three different grids evaluated by varying the mesh size on the entrance face and in the flow direction. The mesh density was refined in the near-wall region over six rows with an expansion ratio of *1.15*. The size of the first row is mentioned for each grid considered.

Face mesh size		Longitudinal mesh size [mm]	Total number of cells
Mean cells size [mm]	Near wall cells size [mm]		
0.4	*0.1*	*0.4*	*1 371 840*
0.3	*0.075*	*0.3*	*3 082 560*
0.17	*0.0425*	*0.17*	*15 143 040*

Table 1 Grids description

To check the mesh sensitivity, a global analysis is carried out: the friction coefficient and the Nusselt number are calculated for the three grids. Table 2 gives the evolution of these two parameters.

Grid	*f*	*Nu*
Coarse	*0.77*	*28.46*
Medium	*0.79*	*27.22*
Thin	*0.82*	*27.05*

Table 2 Grid sensitivity study results

The grid convergence study method proposed by Celik et al. [20] was used to evaluate the mesh independency. For the Nusselt number and the friction coefficient, the grid convergence index (*GCI*) was calculated for the thinnest mesh, as stated in [20]. For the Nusselt number, a *GCI* of *0.01%* was found while a *GCI* of *2.01%* was found for the friction coefficient. Thus, the uncertainty in the thinner mesh is *2.01%*. The approximate relative error between the thin and medium meshes is quite low (it is below *0.7%* for the Nusselt number and *5.5%* for the friction coefficient).

To ensure the mesh size independence, the convergence of the local evolution of *f* and *Nu* was also checked. To do so, both parameters were calculated for each deformation period of each mesh. The results given by the medium grid and the thinnest grid are found to follow the same trend. The maximum difference is lower than *8%* for the friction coefficient and the Nusselt number while the average difference lies around *5.5%* for the friction and around *3.5%* for the heat transfer. The mesh convergence study on the present tube therefore shows that the medium grid allows getting acceptable results without severely increasing the calculation time. Moreover, when the wall deformation is less severe, most of the cases result converges with the same accuracy for a smaller number of cells.

For the following calculations, the medium mesh size was thus chosen, corresponding to a mean cell size of *0.3mm*.

FLOW STRUCTURE

To give a first insight about the effect of the wall deformation parameters on the flow, local variable distributions are studied for the three different tubes. The deformation wavelength is kept constant as the amplitude varies. A more complete study of the influence of the amplitude and also of the wavelength on the tube performances will be discussed in the next section.

Wall deformations are found to induce a particular flow pattern. Successive vortical macrostructures are generated inside the flow, with their main axis aligned with the flow direction. Those structures induce a secondary radial flow which exhibits centripetal and centrifugal velocity components. On Figure 3(a), the main radial velocity vectors on the centripetal and centrifugal directions are identified and sketched at the beginning of a given deformation wavelength and at its centre. The length of each arrow on Figure 3(a) is proportional to the corresponding vectors magnitude. A global flow pattern can thus be drawn for the whole deformation wavelength and is presented on Figure 3(b). Downwash and upwash movements can therefore be spotted, making the boundary layers thickness locally increasing and decreasing. The heat transfer can be enhanced in the near wall region because a better mixing can be achieved.

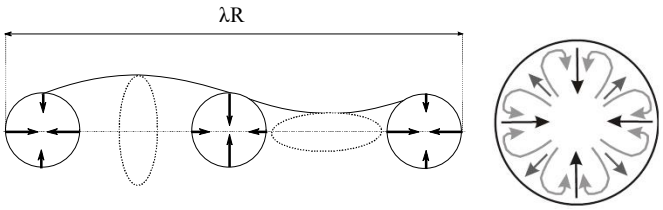

(a) Main radial velocity vectors direction over one deformation wavelength

(b) Global flow movement over one deformation wavelength

Figure 3 Deformed tube radial flow pattern

To evaluate the influence of the deformation parameters on the flow pattern, three tubes with the same wavelength $\lambda = 6$ but different amplitude: *A=12.5%, 30%* and *60%* were studied. Figures 4(a), 4(b) and 4(c) respectively show the radial velocity vector field and the temperature distribution on the same figure for the three tubes. Data were taken at the tube outlet (for the axial coordinate $X=14\lambda R$). Accordingly with the flow pattern identified on Figure 3, it is first worth noting that the temperature distribution is quite different from the one observed for a smooth tube in the laminar regime. The shape of the temperature contours also changes along the tube deformation, as it is much more convoluted for the most deformed tube. It is clear from Figure 4 that the heat transfer improves as the deformation amplitude increases since the mean temperature visibly decreases and the thermal boundary layers become thinner. Moreover, the magnitude of the radial velocity vectors also increases on the whole cross-section. Thus a bigger mechanical loss should also be expected for the most deformed tube.

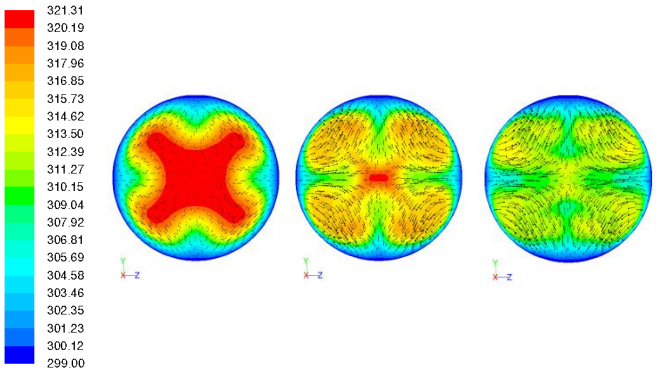

(a) *A=12.5%* (b) *A=25%* (c) A=*60%*

Figure 4 Temperature distribution and radial velocity vectors at the outlet of three deformed tube configuration, λ=6

Those first qualitative results show that the deformation parameters may have a significant impact on the thermo-hydraulic performances observed. The object of the next section is thus to find the optimal deformation amplitude and wavelength by further investigation and quantify their effects on the temperature and velocity fields. The analysis was performed on a global scale and by following the friction and the heat transfer streamwise evolution.

PARAMETRIC STUDY

Influence of the Amplitude

For a given Reynolds number, six tubes with different deformation amplitudes were numerically studied. All the tubes have the same length, *420mm*, and the same deformation wavelength, $\lambda=6$. The amplitude A takes the values *12.5, 25, 30, 40, 50* and *60%*. No bigger deformation amplitude is considered since it would lead to unrealisable geometries. To get a reference, simulations were also conducted for a smooth circular tube ($A = 0\%$). Figure 5 presents the global friction coefficient and the Nusselt number of each tube versus the deformation amplitude. Results show that the larger the deformation amplitude is, the higher the heat transfer is within the tube. Friction also increases with the amplitude. Since the tube wavelength λ is identical for the six deformed tubes, the evolution of Nu and f can also be observed versus the ratio λ/A. When λ/A increases, meaning the deformation is less and less severe, the friction coefficient decreases (Figure 5(a)). In accordance with equation (2), when λ/A increases, mixing time also increases, hence mixing is expected to be less important inside the flow and the convective heat transfer decreases just as it can be seen in Figure 5(b).

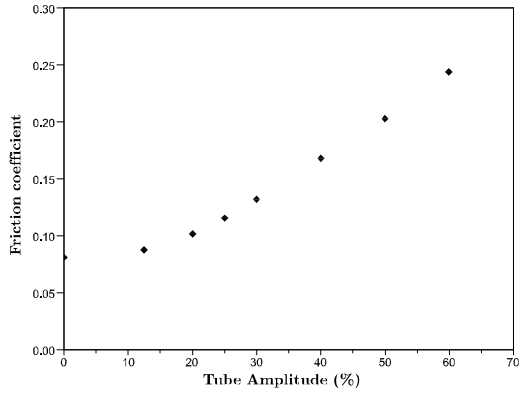

(a) Friction coefficient

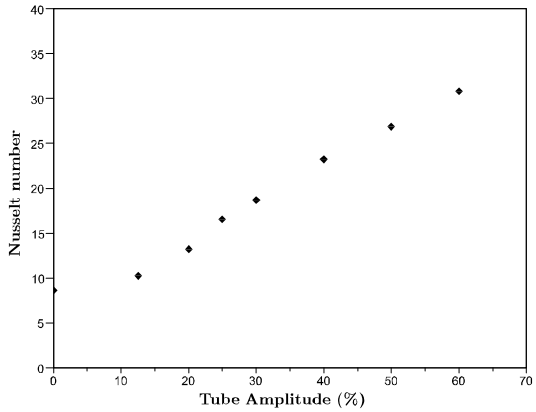

(b) Nusselt number

Figure 5 Evolution of the global friction and heat transfer vs. the deformation amplitude

A calculation of each configurations efficiency as defined by equation (1) is given in Table 3 and shows that over the studied length, with a wavelength $\lambda=6$, the best amplitude A appears to be between *25%* and *30%*. The most appropriate value for the parameter λ/A should therefore lie between *20* and *24*.

A (%)	0	12.5	20	25	30	40	50	60
η	*1*	*1.10*	*1.26*	*1.34*	*1.33*	*1.30*	*1.25*	*1.19*

Table 3 Heat transfer efficiency calculated over *420mm* for different deformation amplitudes

Entrance Length and Local Performances

To get a better understanding of the convective heat transfer mechanisms involved inside the tube, the friction coefficient and the Nusselt number were calculated over each deformation period. Thus, the evolution of these parameters can be observed in the flow direction, from the inlet to the tube outlet. In Figure 6, data from the six tubes with different deformation amplitude depicted in the above paragraph and from the smooth reference tube were displayed. It was found that all the deformed tubes give higher values than the smooth tube for the friction coefficients and the Nusselt numbers but their evolution is different, depending on the tubes deformation. For most of the tubes, friction decreases and reaches a nearly constant value after a very short length (around six periods), whereas, it takes a larger number of periods, closer to nine or ten, for the Nusselt number to get stabilized. For the most severely deformed tubes, the heat transfer is very high for the first period and then decreases drastically to increase a few periods later. At the tubes entrance, the boundary layers are very thin, explaining the high value for the heat transfer. Then the progressive development makes the heat transfer to decrease before rising again due to the macrostructures development and the flow pattern establishment. It is worth noting that for a smooth tube, the friction coefficient reaches the theoretical value $f_{th}=64/Re=0.077$. The Nusselt number also decreases towards the theoretical Nusselt number for a fully established flow in a tube with a circular cross-section and with a constant wall temperature $Nu_{th}=3.74$.

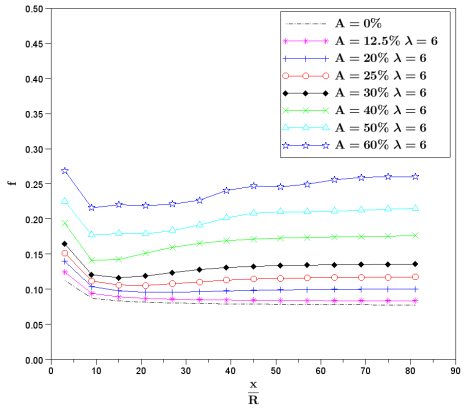

(a) Friction coefficient

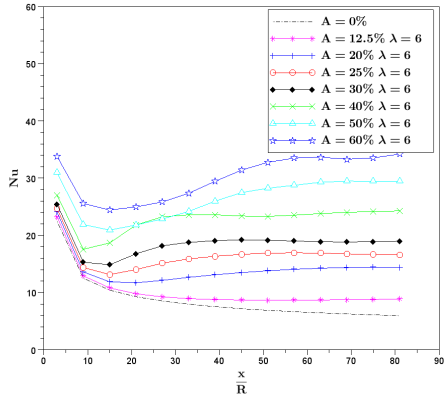

(b) Nusselt number

Figure 6 Friction coefficient and Nusselt number for each deformation period of tubes with different deformation amplitude

From the above observations, a typical entrance length for each tube can be determined. It is defined as the length needed by the flow to become fully thermally and hydrodynamically established. The analysis of the heat transfer and the friction on each tube spatial periods is used to assess the entrance length. To get an approximation of this length, the flow is considered fully developed when the Nusselt number and the friction coefficient reach a constant value, i.e. when the variation becomes less than 2%. As a result, three kinds of behaviour can be identified for the studied tubes:

- Firstly, tubes with a low deformation amplitude (*A=12.5%*) which are quite similar to the smooth circular tube: the flow gets hydrodynamically established around the fourth period and the Nusselt number decreases before reaching a constant value around the ninth period. This type of slightly deformed tube gives better results than the smooth tube but the entrance length remains quite long.
- The second kind of behaviour that can be highlighted corresponds to tubes with medium deformation amplitude (*A* between *20%* and *40%*). These tubes give the best values for the efficiency factor η as it can be seen on Table 3. The friction coefficient and the Nusselt number reach a constant value rapidly: it takes between six and nine periods, depending on the tube considered. Compared with the smooth tube, the heat transfer and the friction are highly enhanced and the entrance length is shortened.
- The last tube category corresponds to highly deformed tubes (*A* between *50%* and *60%*). For these amplitudes, the entrance length is seemingly longer. The flow gets thermally and hydrodynamically established after the eleventh period. Thermo-hydraulic performances are better but the entrance length is significantly longer.

The global analysis presented in the previous section was performed on short tubes. The entrance length may thus have a strong influence on the global efficiency factors calculated in this previous section. From the results presented in Figure 6, it can be seen that the thermo-hydraulic performances are better in the established region of the tube. Therefore, it seems now pertinent to evaluate also the tubes performances in the established regime. The efficiency is evaluated for a fully developed flow in both the deformed tube and the smooth tube: it is calculated over the last twenty deformation wavelength of 1.98m long simulated tubes (corresponding to 66 deformation wavelength). For the *25%* amplitude tube, an efficiency $\eta=2.94$ is calculated whereas *1.34* was found for the *420mm* long tube. It can be clearly seen that the entrance length detrimental effect strongly influence the short tube global performances. For a long tube where the establishment region is negligible, an increase of nearly *200%* of the performances can although be expected.

The same study has been performed with tubes with the same amplitude and different wavelengths. Similar results and trends were achieved and are thus not presented in the current paper.

Influence of the Ratio λ/A

An interesting point is now to check if the parameter λ/A is the geometrical governing parameter for the tube performance, as it was supposed by equation (2). Five tubes with different geometries but the same ratio λ/A were thus studied. Their deformation amplitude and wavelength are summarized in Table 4. The present work considers tubes with $\lambda/A=20$ and is focused on the local performances analysis (for each deformation wavelength). All the five tubes are studied over the same length equal to *420mm*.

Amplitude *A*	Wavelength λ
15%	*3*
25%	*5*
30%	*6*
35%	*7*
45%	*9*

Table 4 Tube deformation parameters

Figure 7 shows the evolution of the friction coefficient and the Nusselt number for each period of each tube. When the deformation amplitude is too low (*A=15%*), the parameters evolution is similar to a smooth reference tube. The global efficiency remains near the value one and the results obtained are comparable to those given by tubes with a ratio *λ/A* larger than *20*. For bigger deformation amplitudes, although the entrance length is not the same for each, all the tubes seem to reach a similar value for the friction coefficient and the Nusselt number in the established regime. All the tubes have the same asymptotic behaviour. Considering these results, *λ/A* seems a rather adequate parameter to consider when studying the deformed tube performance in the established regime.

For tubes long enough, i.e. where the entrance length effect can be neglected, tubes with the same deformation ratio shall give the same results. As for shorter tubes where the entrance length must be taken into account, the present results seem to show that the entrance length effect decreases mainly with *λ*, as long as the amplitude remains high enough. Therefore the deformation configuration must be chosen accordingly: depending of the device length, the influence of the establishment region and thus the deformation parameters is more or less important.

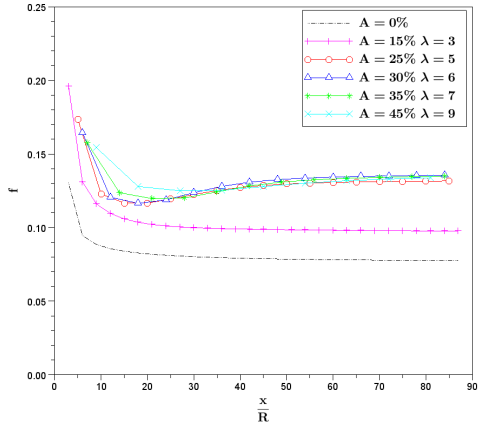

(a) Friction coefficient

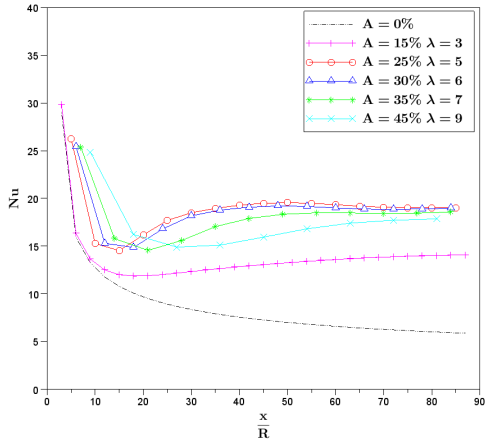

(b) Nusselt number

Figure 7 Friction coefficient and Nusselt number for each deformation period of tubes with the same ratio *λ/A*

CONCLUSION

In the present study, numerical simulations are carried out to analyse the flow thermo-hydraulic characteristics within a tube with successive gradual alternate deformations of its cross-sections as described in [18]. The influence of the deformation amplitude and wavelength are investigated, showing that an optimal configuration can be found. For all the studied tubes, the increase of the global Nusselt number is higher than the increase of the friction coefficient.

The organisations of the flow inside the deformed tubes are strongly dependant on the deformation parameters: important vortical macrostructures appear inside the flow, leading to different wall heat transfer enhancement.

The deformation ratio *λ/A* is found to be an appropriate parameter to qualify a tube heat transfer enhancement when the flow is fully developed whereas the variation of the deformation wavelength and the deformation amplitude affect the establishment length. The optimal range for *λ/A* seems to lie between *20* and *24* at the studied Reynolds number.

The entrance lengths of the tubes are also dependant from the deformation geometrical parameters. The lower performances of the established region must be taken into account for short tubes since they significantly affect the global performances. Therefore, the choice of the best deformation parameters depends of the practical application considered and the global tube length.

The present study gives an optimal value for the deformation parameter *λ/A* at a given Reynolds number. If the Reynolds number varies, whether the optimal configuration remains the best one should be further investigated.

REFERENCES

[1] Timite B., Castelain C., Peerhossaini H., Mass transfer and mixing by pulsatile three-dimensional chaotic flow in alternating curved pipes, *International Journal of Heat and Mass Transfer,* Vol. 54,2011, pp. 3933-3950

[2] Webb R. L., Principles of Enhanced Heat Transfer, John *Wiley & Sons, Inc*., 1994

[3] Kumar V., Nigam K., Laminar convective heat transfer in chaotic configuration, *International Journal of Heat and Mass Transfer,* Vol. 50, 2007, pp. 2469-2479

[4] Chagny C., Castelain C., Peerhossaini H., Chaotic heat transfer for heat exchanger design and comparison with a regular regime for a large range of Reynolds numbers, *Applied Thermal Engineering*, Vol. 20, 2000, pp.1615-1648

[5] Habchi C., Lemenand T., Della Valle D., Peerhossaini H., Liquid/liquid dispersion in a chaotic advection flow, *International Journal of Multi-phase Flow*, Vol. 35, 2009, pp. 485-497

[6] Habchi C., Lemenand T., Della Valle D., Peerhossaini H., Alternating mixing tabs in multifunctional heat exchanger-reactor, *Chemical Engineering and Processing*, Vol. 49, 2010, pp. 653-661

[7] Habchi C., Russeil S., Bougeard D., Harion J. H., Lemenand T., Della Valle D., Peerhossaini H., Enhancing heat transfer in vortex generator-type multifunctional heat exchangers, *Applied Thermal Engineering*, Vol. 38, 2012, pp. 14-25.

[8] Yerra K. K., Manglik R. M., Jog M.A., Optimization of heat transfer enhancement in single-phase tube side flows with twisted-tape inserts, *International Journal of Heat Exchangers*, Vol. 8, 2007, pp. 117-138

[9] Barba A., Rainieri S., Spiga M., Heat transfer enhancement in a corrugated tube, *International Communications in Heat and Mass Transfer*, Vol. 39, 2002, pp. 313-322
[10] Rainieri S., Pagliarini G., Convective heat transfer to temperature dependent property fluids in the entry region of corrugated tubes, *International Journal of Heat and Mass Transfer*, Vol. 45, 2002, pp. 4525-4536
[11] Rainieri S., Bozzoli F., Pagliarini G., Experimental investigation on the convective heat transfer in straight and coiled corrugated tubes for highly viscous fluids: Preliminary results, *International Journal of Heat and Mass Transfer*, Vol. 55, 2012, pp. 498-504
[12] Mahmud S., Islam A. K. M. S., Feroz C. M., Flow and heat transfer characteristics inside a wavy tube, *Heat and Mass Transfer*, Vol. 39, 2003, pp. 387-393
[13] Bishara F., Jog M. A., Manglik R. M., Heat transfer and pressure drop of periodically fully developed swirling laminar flows in twisted tubes with elliptical cross-section, *ASME (Ed.), Heat transfer, Fluid flows and Thermal systems*, Vol. 9, Lake Buena Vista, Florida, pp. 1131-1137
[14] Meng J. A., Liang X. G., Chen Z. J., Li Z. X., Experimental study on convective heat transfer in alternating elliptical axis tubes, *Experimental Thermal and Fluid Science*, Vol. 29, 2005, pp. 457-469
[15] Chen W. L., Fang L. C., A numerical study on the flow over a staggered oval tube for heat-transfer enhancement, *Journal of the Chinese Society of Mechanical Engineers*, Vol. 25, 2004, pp. 209-216
[16] Chen W. L., Guo Z., Chen C. K., A numerical study on the flow over a novel tube for heat-transfer enhancement with a linear eddy-viscosity model, *International Journal of Heat and Mass Transfer*, Vol. 47, 2004, pp. 3431-3439
[17] Chen W. L., Wong K. L., Huang C. T., A parametric study on the laminar flow in an alternating horizontal or vertical oval cross-section pipe with computational fluid dynamics, *International Journal of Heat and Mass Transfer*, Vol. 49, 2006, pp. 287-296
[18] Harion J. L., Bertin J. L., Bahadori B., Mixing and heat transfer increase in a tube with alternate successive deformations, *W. H. E. W. P. Hahne, K. Spindler (Eds.), 3rd European Thermal Sciences Conference 2000*, Vol. 1, Edizioni ETS, 2000, pp. 331-336
[19] ANSYS Fluent 12.0 User's guide, 2009
[20] Celik I. B., Ghia U., Roache P. J., Freitas C. J., Coleman H., Raad P. E., Procedure for Estimation and Reporting of Uncertainty Due to Discretization in CFD Applications, *Journal of Fluids Engineering*, Vol. 130, 2008, pp. 0780011-0780014